congenital cataract, 51.3 % with white pupil, 40.9 % with cataract found with other diseases, 33.3 % with poor visual fixation, 32.3 % with cataract diagnosed by previous physicians, 28.6 % with nystagmus, 13.3 % with photophobia, 8.0 % with strabismus, and 1.4 % with poor vision.

The timing of first visit to ophthalmologists was earliest for those with nystagmus (5.4 ± 4.3 months) followed by, in descending order, poor visual fixation (9.0 ± 8.7 months), white pupil (9.7 ± 21.2 months), family history (10.8 ± 21.7 months), cataract diagnosed with other diseases (11.1 ± 19.9 months), photophobia (29.2 ± 14.5 months), strabismus (38.2 ± 34.3 months), cataract diagnosed by previous physicians (47.4 ± 69.4 months), and poor vision (81.3 ± 46.8 months).

Family history and other variables

Because more than 98 % of unilateral cases had no family history, the relationship between family history and other variables were analyzed for bilateral cases.

The average age at initial visit for cases with family history was 2.5 ± 3.4 years whereas that for cases without family history was 2.5 ± 3.6 years (no significant difference; Student t test, $p = 0.851$). The incidence of associated ocular anomalies did not differ between the two groups (15.4 vs. 15.7 %). The prevalence of associated systemic problems was significantly lower among cases with family history (5.8 %) than among those without (35.7 %) ($p < 0.0001$).

Cataract morphology

Because cataract morphology for both eyes was similar for more than 90 % of bilateral cases, analysis was based on the number of cases rather than the number of eyes, after exclusion of those for which valid information was not available.

The common morphological type of cataract included total cataract (29.3 %), nuclear cataract (19.4 %), and lamellar cataract (18.5 %) in bilateral cases whereas posterior subcapsular/polar cataract (34.7 %), nuclear cataract (23.5 %), and total cataract (21.8 %) were frequently found in unilateral cases. These numbers were calculated including those with unknown and other type of cataract, and thus are different from those shown in Table 4.

Bilateral and unilateral cases were compared after excluding cases with unknown type, bilaterally different type, and other type of cataract (Table 4). The percentage of total ($p < 0.05$) and lamellar cataracts ($p < 0.05$) was significantly greater among bilateral cases whereas posterior subcapsular/polar cataracts were more frequent in unilateral cases ($p < 0.05$).

Cataract morphology and other variables

Age at initial visit is plotted as a function of cataract morphology in Fig. 1. Cases with anterior subcapsular/polar cataract visited the physician earliest, followed by those with total, nuclear, combined, lamellar and posterior subcapsular/polar cataracts. Statistical analysis revealed that age at initial visit was significantly lower for patients with anterior subcapsular, total, and nuclear cataract than for those with lamellar and posterior subcapsular cataract ($p < 0.05$, Kruskal–Wallis test, Scheffe multiple comparison).

For cases with total cataract, age at the initial visit was significantly lower for bilateral (12.3 ± 21.3 months) than unilateral cases (25.7 ± 34.4 months) ($p = 0.0314$, Welch t-test). Such differences were not found for cases with other cataract morphology.

The relationship between cataract morphology and family history was analyzed for bilateral cases. Family history was found in 30.6 % of cases with total opacity, 27.1 % of cases with lamellar opacity, 44.8 % of cases with nuclear opacity, 41.2 % of cases with posterior subcapsular/polar opacity, 33.3 % of cases with anterior subcapsular/polar opacity, 43.8 % of cases with combined opacity, 21.2 % of cases with a different type of opacity bilaterally, and 28.6 % of cases with another type of opacity. These percentages were not statistically significantly different.

Table 4 Cataract morphology

Percentages are calculated after excluding cases with bilaterally different type, other type, and unknown type of cataract, to compare bilateral and unilateral cases

n.s. not significant

* Bilateral and unilateral cases were compared by use of the χ^2 test

Morphology	Bilateral cases	Unilateral cases	p value*
Total	95/281 (33.8 %)	37/169 (21.9 %)	$p < 0.05$
Lamellar	60/281 (21.4 %)	11/169 (6.5 %)	$p < 0.05$
Nuclear	63/281 (22.4 %)	40/169 (23.7 %)	n.s.
Posterior capsular/polar	23/281 (8.2 %)	59/169 (34.9 %)	$p < 0.05$
Anterior capsular/polar	6/281 (2.1 %)	5/169 (3.0 %)	n.s.
Combined	34/281 (12.1 %)	17/169 (10.1 %)	n.s.
Different bilaterally	37/343	–	–
Others	6/343	1/178	–
Unknown	19/343	8/178	–

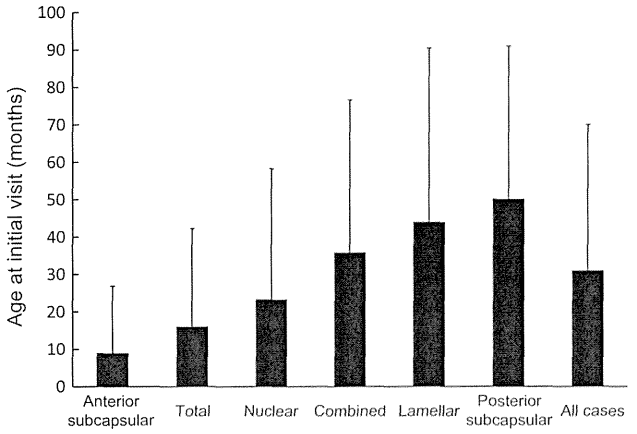

Fig. 1 Age at initial visit (months) as a function of cataract morphology

There was no significant association between cataract morphology and prevalence of associated systemic disorders. For cases with total cataract, the incidence of systemic disorders was 37.6 % among bilateral cases and 15.6 % among unilateral cases, which was significantly different ($p = 0.022$). For cases with nuclear cataracts, the incidence of systemic abnormalities was significantly higher for bilateral cases (32.8 %) than for unilateral cases (2.9 %) ($p = 0.0007$). Such differences were not found for cases of cataracts with a different morphology.

The relationship between cataract morphology and incidence of associated ocular comorbidities was assessed (Table 5). It was found that cases with total cataracts were frequently associated with strabismus, nystagmus, and microphthalmos whereas nuclear cataract cases presented high prevalence of microcornea. Persistent fetal vasculature and posterior lenticonus were more often seen for eyes with posterior subcapsular/polar cataract than for those with other cataract morphology.

Presumed etiology of congenital cataract

The etiology was estimated from the data provided by the survey and classified into several categories, including hereditary, congenital ocular abnormality, congenital systemic diseases, and unknown (Table 6). Whenever family history of congenital/developmental cataract was positive, it was judged to be hereditary.

Among 343 bilateral cases, unknown etiology (idiopathic) was most common among 123 cases (35.9 %), followed by hereditary (104 cases, 30.3 %), systemic anomalies (80 cases, 23.3 %), and congenital ocular abnormality (26 cases, 10.5 %).

Among 178 unilateral cases, the presumed etiology was unknown for 121 (68.0 %), congenital ocular abnormality for 38 cases (21.3 %), systemic diseases for 17 cases (9.6 %), and hereditary for 2 cases (1.1 %).

Table 6 Presumed etiology of congenital cataract

Etiology	Bilateral cases	Unilateral cases
Hereditary (family history)	104 (30.3 %)	2 (1.1 %)
Congenital ocular abnormality	36 (10.5 %)	38 (21.3 %)
Persistent fatal vasculature	3	14
Nanophthalmos	11	6
Microcornea	12	5
Others	10	13
Systemic diseases	80 (23.3 %)	17 (9.6 %)
Chromosomal disorder		
Down syndrome	24	4
Others	4	3
Intrauterine infection		
Rubella	2	1
TORCH	1	0
Central nervous system abnormality		
Mental retardation	6	0
Epilepsy	6	0
Others	13	0
Cardiac anomaly	10	1
Low birth weight	6	3
Other systemic diseases	8	5
Unknown	123 (35.9 %)	121 (68.0 %)
Total	343	178

Table 5 Frequently associated ocular comorbidities and cataract morphology

Ocular diseases	Bilateral cases	Unilateral cases
Strabismus	Total, different bilaterally	Nuclear
Nystagmus	Total	–
Microcornea	Nuclear	–
Microphthalmos	Anterior subcapsular/polar, total	Total
Persistent fetal vasculature	Posterior subcapsular/polar	Posterior subcapsular/polar
Posterior lenticonus	Posterior subcapsular/polar	–

Discussion

This study population was confined to those undergoing surgical treatment for congenital/developmental cataracts; patients whose surgical intervention was not indicated were not included. This was because, when planning this retrospective study, we believed that more detailed clinical data would be available for surgical cases than for non-surgical cases. Thus, it should be noted that these results do not necessarily give a complete picture of cases with congenital/developmental cataract in general. Cases with unilateral dense cataracts diagnosed too late for surgery and those with severe preexisting ocular anomalies contraindicated to cataract surgery were not included in this study. Likewise patients with severe systemic comorbidities at a high risk of developing complications in general anesthesia were excluded from the current study population. Nevertheless, another study among facilities similar to those in this study showed that more than 85 % of respondents will recommend surgery for congenital cataract even when visual prognosis may not be very promising, after fully explaining the pros and cons of surgery to the patients' family. Therefore, we believe that the results obtained herein do not deviate substantially from the overall situation for congenital/developmental cataracts in Japan.

Laterality

In 2000, Rahi et al. [12] studied 243 cases with congenital cataracts in the UK and reported that 66 % were bilateral. A Danish study by Haargaard et al. [13] in 2004 reported that 64 % of 1,027 congenital cataracts were bilateral, and an Australian study by Wirth et al. in 2002 found that 56 % of 421 cases had cataracts in both eyes [14]. These studies were conducted nationwide and/or across wider regions, and their results are in good agreement with ours. Smaller-scale studies, however, report different results. Eckstein et al. [15] investigated 366 cases in India and reported an incidence of bilateral cases of 78.1 %, of which 15 % were caused by rubella; Jain et al. [16] reported that 92.1 % of 76 congenital cataracts were bilateral. SanGiovanni et al. [17] stated that 47.9 % of 73 congenital cataracts in the USA were bilateral. Judging from previous large-scale studies and our current results, it seems that the ratio of bilateral and unilateral cases in congenital cataract is approximately 2:1.

Family history of congenital cataract

We found that family history was significantly higher for bilateral cases (33.1 %) than for unilateral cases (1.3 %), in good agreement with results reported by Rahi et al. [12] and Haargaard et al. [13].

Associated systemic diseases

Consistent with our results, Rahi et al. [12] and Haargaard et al. [13] reported that the incidence of associated systemic comorbidities was higher for bilateral cases than for unilateral cases.

Associated systemic anomalies were found for 35.7 % of patients without a family history of congenital cataract, compared with only 5.8 % of those with family history. The prevalence of preexisting ocular problems was not associated with family history of congenital cataract, however. These results suggest that many patients with hereditary congenital cataract have no concurrent systemic and ocular diseases other than cataract. Haargaard et al. [13] also reported that 91 % of cases with hereditary congenital cataract had no abnormality other than cataract (isolated cataract).

Associated ocular diseases

We found that strabismus accompanied congenital/developmental cataracts among 33.3 % of patients, which is consistent with results from previous studies, for example 24.1 % reported by Deweese [18], 33.6 % reported by Yang et al. [19], and 28 % reported by Kim et al. [20].

The incidence of nystagmus associated with congenital cataract varies: 22.6 % reported by Deweese [18], 38.1 % reported by Yang et al. [19], and 15 % reported by Kim et al. [20]. Our results (17.7 %) fall within this range.

The prevalence of microphthalmos associated with congenital cataract was reported to be 4.5 % by Deweese [18] and 6.6 % by Rahi et al. [12]. The prevalence of either microphthalmos or microcornea was reported to be 3.9 % by Haargaard et al. [13], and the prevalence of microcornea was 10.8 % among cases in the study by Yang et al. [19]. In many of these studies, microphthalmos and microcornea are not distinguished clearly. In this study, we found microphthalmos in 3.6 % and microcornea in 6.0 % of cases. When combined, either microphthalmos or microcornea was present in 8.6 % (45/521).

Persistent fetal vasculature often coexists with congenital cataract, and its incidence is reported to be 3.8 % by Yang et al. [19], 5.7 % by Haargaard et al. [13], 8.2 % by Rahi et al. [12], 4.3 % by Ledoux et al. [21], and 3.0 % by Plager et al. [22] The prevalence found in our study, 2.0 %, is somehow lower than in these reports.

The incidence of posterior lenticonus in eyes with congenital cataracts varies substantially, depending on the study: 0.9 % reported by Haargaard et al. [13], 10.1 % by Ledoux et al. [21], and 14.9 % by Plager et al. [22]. In our study, 1.5 % of cases presented with posterior lenticonus. These discrepancies may be because of different study populations, different surgical procedures, and/or timing of

diagnosis. Diagnosis of posterior lenticonus is sometimes difficult before surgery, because of dense opacity, and even during surgery, when the lens is being removed by use of the pars plana lensectomy technique. In fact, one of the authors (TN) found posterior lenticonus in 9.8 % (6/61) of cases during surgery in which limbal approach technique with implantation of an intraocular lens was scheduled.

Concomitant ocular abnormalities, for example strabismus, persistent fatal vasculature, and posterior lenticonus, are more frequently associated with unilateral rather than bilateral cases of congenital cataract. For persistent fatal vasculature, Haargaard et al. [13] reported prevalence of 15.0 vs. 0.5 % (unilateral vs. bilateral, $p < 0.0001$) and Rahi et al. [12] reported 21.7 vs. 1.3 % ($p < 0.0001$). The incidence of posterior lenticonusis was reported to be 1.9 vs. 0.3 % ($p = 0.025$) by Haargaard et al. [13]. For the association of microphthalmos with congenital cataract, Rahi et al. [12] reported no difference between unilateral and bilateral cases (7.2 vs. 6.3 %, $p = 0.770$) whereas Haargaard et al. [13] reported that the prevalence of either microphthalmos or microcornea among patients with congenital cataracts was significantly larger for unilateral (5.9 %) than for bilateral (2.8 %) cases ($p = 0.0127$). We found the incidence of microphthalmos and microcornea to be no different between bilateral and unilateral cases.

Age at initial visit

In this study, age at the first visit to ophthalmologists averaged 2.6 ± 3.3 years (mean ± standard deviation; range 0 to 18.8 years). Yang et al. [19] reported an average age of 2 years 1 month (0–10 years 1 month) and Haargaard et al. [13] reported a medium age of 3 years; both results are very similar to ours. Patients in the UK were, however, examined and diagnosed at a very early stage, average 8 weeks (0–15 years) after birth, as reported by Rahi et al. [12]. This is because of the national ophthalmic surveillance scheme in the UK, administered ophthalmologists and pediatricians, in which all British pediatricians are required to conduct ocular examinations of newborns; screening by pediatricians and treatment by ophthalmologists are free of charge; and 89 % of ophthalmologists participate in the national survey of congenital/infantile cataracts and report to the registry [12].

There is a specific critical period for surgical treatment of congenital cataract to achieve optimum orthoptics. For unilateral cases, the report of 6 weeks from birth by Birch et al. [8] is widely accepted. For bilateral cases, there are several opinions, ranging from 8 [9] and 10 [10] to 14 weeks [11] from birth; we adopted 12 weeks as the threshold for this analysis. We found that only 15.2 % (25/165 cases) of unilateral cases and 31.4 % (103/328 cases) of bilateral cases were seen for the first time within the critical visual period, indicating that detection and diagnosis of congenital cataracts were too late in many cases.

The relationship between main complaint and age at the initial visit was analyzed. For bilateral cases, 64.3 % with a family history of congenital cataracts visited within 12 weeks, followed by 51.3 % with white pupil, and 40.9 % with cataract diagnosed with other eye diseases. For unilateral cases, the percentage of patients who saw a physician within the critical period was 42.6 % for those with white pupil and 28.6 % for those with cataract diagnosed with other eye diseases, compare with 0 % for other main complaints. Thus, two-thirds of the patients with family history visited within the critical period, and fewer than half of those with white pupil came to see a doctor within that period.

When studying the relationship between cataract morphology and age at initial visit, it was found that patients with total, anterior subcapsular, and nuclear opacity visited a physician significantly earlier than those with posterior subcapsular and lamellar opacity. This seems to be because total, anterior subcapsular, and nuclear cataract are often apparent from white pupils at an earlier stage, in contrast with posterior subcapsular and lamellar cataract.

Main complaints

Few studies have investigated the main complaints of patients with congenital/developmental cataract. Yang et al. [19] reported the distribution of initial presentations of suspected cataract: poor visual acuity or complaint of blurred vision for 33.3 %, white pupil for 31.5 %, discovery on screen test by pediatricians or at school for 19.8 %, squint for 10.8 %, eye shaking for 2 %, head tilt for 1.5 %, and photophobia for 1 %. The percentages of white pupil and squint in their report are similar to our results, but those of nystagmus and photophobia are inconsistently lower; the reason for this is currently unknown.

Cataract morphology

There are a variety of reports on the distribution of morphological types of cataract. Haargaard et al. [13] found nuclear or lamellar cataract among 34 %, total cataract among 15 %, posterior subcapsular cataract among 14 %, combined cataract among 10 %, posterior polar cataract among 10 %, anterior polar cataract among 6 %, others among 8 %, and unknown among 3 %. Compared with their results, we found a somewhat higher proportion of total cataracts and a lower proportion of posterior subcapsular/polar and anterior subcapsular/polar cataracts.

Yang et al. [19] reported a very high frequency of nuclear cataracts (48.4 %) compared with total (22.4 %),

posterior polar (13.8 %), and lamellar (8.5 %) cataracts. Plager et al. [22] found lamellar among 35.8 % of cases, nuclear among 16.4 %, posterior subcapsular/polar among 38.8 %, total among 6.0 %, and anterior polar cataract among 1.5 %. Ledoux et al. [21] state that lamellar opacity was present among 30.9 %, nuclear among 24.5 %, posterior subcapsular among 14.4 %, posterior lenticonus among 10.1 %, posterior polar among 7.9 %, total among 2.9 %, anterior polar opacity among 2.9 %, and others among 2.2 %. These conflicting results seem suggestive of different surgical indications for congenital cataracts, and diverse background of patients, for example age, ethnicity, and socioeconomic situations.

The distribution of cataract morphology did not differ substantially between those with and without family history of congenital cataracts, indicating that inherited and non-inherited congenital cataracts are no different in their phenotype. Haargaard et al. [13]. stated that hereditary cataracts tend to be more associated with nuclear and lamellar cataracts, whereas idiopathic types are more likely to be linked with posterior subcapsular/polar cataracts, but they did not show a statistically significant difference between them.

There is no study of the relationship between cataract morphology and the incidence of ocular comorbidities. We found that cases with total cataract were frequently associated with strabismus, nystagmus, and microphthalmos whereas persistent fetal vasculature and posterior lenticonus were more often seen for eyes with posterior subcapsular/polar cataracts than for those with other cataract morphology. These results can be explained by the fact that total cataract results in more severe visual deprivation, leading to strabismus and nystagmus at an early stage, whereas posterior fetal vasculature and posterior lenticonus are anatomically related to posterior subcapsular/polar cataracts.

Presumed etiology of congenital cataract

The distribution of presumed etiology in this study is in good agreement with that reported by Rahi et al. [13], who reported that 34 % of bilateral cases were of unknown etiology, 28 % were hereditary, 25 % were associated with systemic diseases, and 13 % were linked to ocular diseases. They also reported a higher proportion of unilateral cases associated with ocular comorbidities, however [12]. This is because their statistics include unilateral cases with persistent hyperplastic primary vitreous and anterior segment dysgeneses, severe cases of which were excluded from our study population because of the absence of surgical indications. The breakdown of presumed etiology reported by Haargaard et al. [13] is highly consistent with our results for both bilateral and unilateral cases.

In conclusion, we herein report the clinical features of cases with congenital/infantile cataracts who underwent surgical treatment. Understanding the detailed clinical characteristics of these cases and analyzing the relationships among the different variables will be of clinical importance to achieving earlier diagnosis and providing timely treatment of congenital/developmental cataract to prevent potentially treatable amblyopia in children.

Acknowledgments Supported by the Health and Labour Sciences Research Grant, Research on Measures for Intractable Diseases, The Ministry of Health Labour and Welfare, Japan. We thank all physicians who contributed to this study by providing valuable information, those from National Center for Child Health and Development, Hyogo Prefectural Kobe Children's Hospital, Aichi Children's Health and Medical Center, Osaka City General Hospital, Kyorin University School of Medicine, Fukushima Medical University, Osaka Medical Center and Research Institute for Maternal and Child Health, Iwate Medical University, University of Tsukuba Faculty of Medicine, Dokkyo Medical University, Kagoshima University Faculty of Medicine, Kanagawa Children's Medical Center, Hamamatsu University School of Medicine, Osaka University Medical School, Keio University School of Medicine, Kurume University School of Medicine, Wakayama Medical University, Kagawa University Faculty of Medicine, Kanazawa University School of Medicine, University of Fukui Faculty of Medical Science, Shiga University of Medical Science, Ehime University School of Medicine, Toho University Omori Medical Center, Shinshu University School of Medicine, Kyushu University School of Medicine, Kobe University School of Medicine, Nagoya University School of Medicine, Hokkaido Children's Hospital and Medical Center, and Kagawa National Children's Hospital.

Conflicts of interest T. Nagamoto, None; T. Oshika, None; T. Fujikado, None; T. Ishibashi, None; M. Sato, None; M. Kondo, None; D. Kurosaka, None; N. Azuma, None.

References

1. Taylor D. Congenital cataract: the history, the nature and the practice: the Doyne Lecture. Eye. 1998;12:9–36.
2. Gilbert C, Foster A. Childhood blindness in the context of VISION 2020–the right to sight. Bull World Health Organ. 2001;79:227–32.
3. Thylefors B. A global initiative for the elimination of avoidable blindness. Commun Eye Health. 1998;11:1–3.
4. Zetterström C, Lundvall A, Kugelberg M. Cataracts in children. J Cataract Refract Surg. 2005;31:824–40.
5. Lambert SR, Drack AV. Infantile cataracts. Surv Ophthalmol. 1996;40:427–58.
6. Hiles DA, Carter BT. Classification of cataracts in children. Int Ophthalmol Clin. 1977;17:15–29.
7. Hiles DA. Infantile cataracts. Pediatr Ann. 1983;12:556–73.
8. Birch EE, Stager DR. The critical period for surgical treatment of dense congenital unilateral cataract. Invest Ophthalmol Vis Sci. 1996;37:1532–8.
9. Gelbart SS, Hoyt CS, Jastrebski G, Marg E. Long-term visual results in bilateral congenital cataracts. Am J Ophthalmol. 1982;93:615–21.
10. Lambert SR, Lynn MJ, Reeves R, Plager DA, Buckley EG, Wilson ME. Is there a latent period for the surgical treatment of children with dense bilateral congenital cataracts? J AAPOS. 2006;10:30–6.

11. Birch EE, Cheng C, Stager DR Jr, Weakley DR Jr, Stager DR Sr. The critical period for surgical treatment of dense congenital bilateral cataracts. J AAPOS. 2009;13:67–71.
12. Rahi JS, Dezateux C. british congenital cataract interest group. congenital and infantile cataract in the United Kingdom: underlying or associated factors. Invest Ophthalmol Vis Sci. 2000;41:2108–14.
13. Haargaard B, Wohlfahrt J, Fledelius HC, Rosenberg T, Melbye M. A nationwide Danish study of 1027 cases of congenital/infantile cataracts: etiological and clinical classifications. Ophthalmology. 2004;111:2292–8.
14. Wirth MG, Russell-Eggitt IM, Craig JE, Elder JE, Mackey DA. Aetiology of congenital and paediatric cataract in an Australian population. Br J Ophthalmol. 2002;86:782–6.
15. Eckstein M, Vijayalakshmi P, Killedar M, Gilbert C, Foster A. Aetiology of childhood cataract in south India. Br J Ophthalmol. 1996;80:628–32.
16. Jain IS, Pillay P, Gangwar DN, Dhir SP, Kaul VK. Congenital cataract: etiology and morphology. J Pediatr Ophthalmol Strabismus. 1983;20:238–42.
17. SanGiovanni JP, Chew EY, Reed GF, Remaley NA, Bateman JB, Sugimoto TA, et al. Infantile cataract in the collaborative perinatal project: prevalence and risk factors. Arch Ophthalmol. 2002;120:1559–65.
18. Deweese MW. A survey of the surgical treatment of congenital cataracts. Am J Ophthalmol. 1962;53:853–8.
19. Yang ML, Hou CH, Lee JS, Liang YS, Kao LY, Lin KK. Clinical characteristics and surgical outcomes of pediatric cataract in Taiwan. Graefes Arch Clin Exp Ophthalmol. 2006;244:1485–90.
20. Kim KH, Ahn K, Chung ES, Chung TY. Clinical outcomes of surgical techniques in congenital cataracts. Korean J Ophthalmol. 2008;22:87–91.
21. Ledoux DM, Trivedi RH, Wilson ME Jr, Payne JF. Pediatric cataract extraction with intraocular lens implantation: visual acuity outcome when measured at age 4 years and older. J AAPOS. 2007;11:218–24.
22. Plager DA, Kipfer H, Sprunger DT, Sondhi N, Neely DE. Refractive change in pediatric pseudophakia: 6-year follow-up. J Cataract Refract Surg. 2002;28:810–5.

Cell Biology International ISSN 1065-6995
doi: 10.1002/cbin.10174

RESEARCH ARTICLE

Interaction between optineurin and the bZIP transcription factor NRL

Chunxia Wang[1,2,3], Katsuhiro Hosono[1,2], Masafumi Ohtsubo[2], Kentaro Ohishi[2], Jie Gao[1,2], Nobuo Nakanishi[2], Akiko Hikoya[1], Miho Sato[1], Yoshihiro Hotta[1] and Shinsei Minoshima[2]*

1 Department of Ophthalmology, Hamamatsu University School of Medicine, 1-20-1 Handayama, Hamamatsu 431-3192, Japan
2 Department of Photomedical Genomics, Basic Medical Photonics Laboratory, Medical Photonics Research Center, Hamamatsu University School of Medicine, 1-20-1 Handayama, Hamamatsu 431-3192, Japan
3 Department of Ophthalmology, The Fourth Affiliated Hospital of China Medical University, Shenyang 110005, China

Abstract

Although the gene encoding optineurin (OPTN) is a causative gene for glaucoma and amyotrophic lateral sclerosis, it is ubiquitously expressed in all body tissues, including the retina. To study the function of OPTN in retinal ganglion cells as well as the whole retina, we previously isolated OPTN-interacting proteins and identified the gene encoding the bZIP transcription factor neural retina leucine zipper (NRL), which is a causative gene for retinitis pigmentosa. Herein, we investigated the binding between OPTN and NRL proteins in HeLaS3 cells. Co-expression of HA-tagged NRL and FLAG-tagged OPTN in HeLaS3 cells followed by immunoprecipitation and Western blotting with anti-tag antibodies demonstrated the binding of these proteins in HeLaS3 cells, which was confirmed by proximity ligation assay. NRL is the first OPTN-binding protein to show eye-specific expression. A series of partial-deletion OPTN plasmids demonstrated that the tail region (423–577 amino acids [aa]) of OPTN was necessary for binding with NRL. Immunostaining showed that Optn (rat homologue of OPTN) was expressed in rat photoreceptors and localised in the cytoplasm of photoreceptor cells. This is a novel demonstration of Optn expression in photoreceptor cells. OPTN was not detected in photoreceptor nuclei under our experimental conditions. Further analyses are necessary to elucidate the function of OPTN and the significance of its possible binding with NRL in photoreceptor cells.

Keywords: co-immunoprecipitation; NRL; optineurin; photoreceptor; protein interaction; proximity ligation assay

Introduction

The cellular protein optineurin (OPTN) was originally given the name FIP-2 and characterised by its binding of the adenovirus E3 14.7-kDa protein and induction by tumour necrosis factor alpha (Li et al., 1998). OPTN was also described as a huntingtin interacting protein HYPL, a transcription factor IIIA-interacting protein (TFIIIA-intP) (Faber et al., 1998; Moreland et al., 2000), and an NF-κB essential modulator (NEMO)-related protein with the name NRP (Schwamborn et al., 2000). Following the discovery that mutations in the *OPTN* gene were causative for adult-onset primary open-angle glaucoma (POAG), the gene was named optineurin (Rezaie et al., 2002) and OPTN was thought to have a neuroprotective function, which was subsequently supported by studies in limited cell culture systems (De Marco et al., 2006; Chalasani et al., 2007).

OPTN is ubiquitously expressed in tissues, including the heart, brain, skeletal muscle, adrenal cortex and retina (Li et al., 1998; Rezaie et al., 2002). For this reason, OPTN is thought to play roles in various tissues and cell types in addition to retinal ganglion cells to maintain their normal functions. The function of OPTN in tissues other than retinal ganglion cells was exemplified by a recent report that several *OPTN* mutations cause amyotrophic lateral sclerosis (ALS) but not POAG (Maruyama et al., 2010). This discovery supports the neuroprotective function of OPTN not only in the retina but also in the spinal cord.

OPTN expression is seen in ocular tissues such as the trabecular meshwork, non-pigmented ciliary epithelium and retina (Rezaie et al., 2002). Retinal ganglion cells have the highest level of OPTN expression in the retina (Rezaie and Sarfarazi, 2005; Rezaie et al., 2005; Kroeber et al., 2006). To study the general functions of OPTN not only in ganglion

*Corresponding author: e-mail: mino@hama-med.ac.jp
Abbreviations: aa, amino acid; NEMO, NF-κB essential modulator; OPTN, optineurin (human); Optn, optineurin (rat); NRL, neural retina leucine zipper (human); Nrl, neural retina leucine zipper (rat); IP, immunoprecipitation; WB, Western blotting; PLA, proximity ligation assay

cells, but in other types of retinal cells, we isolated cDNA clones of OPTN-binding candidate proteins by yeast two-hybrid screening from a human retinal cDNA library (Ohtsubo et al., unpublished). We found that one of these cDNA clones encodes a neural retina-specific leucine zipper protein, the bZIP transcription factor (NRL). The *NRL* gene is expressed in rod nuclei in adults and has important functions in the differentiation of various types of ocular cells (Mears et al., 2001; Swain et al., 2001). Mutations of the *NRL* gene also cause retinitis pigmentosa (RP) (Bessant et al., 1999).

We report here interactions between OPTN and NRL proteins in cultured cells as well as the expression of Optn in rat photoreceptor cells.

Materials and methods

The study was approved by the Institutional Ethics Committee for Genetic and Genomic Research and the Animal Use Committee of Hamamatsu University School of Medicine.

Antibodies

Rabbit anti-HA-tag antibody (561) was purchased from MBL International Corporation (Woburn, MA), and mouse anti-FLAG M2 monoclonal antibody (F3165) was purchased from Sigma–Aldrich, Japan, K.K. (Tokyo, Japan). We confirmed by Western blot analysis that the anti-HA-tag and anti-FLAG M2 monoclonal antibodies do not cross-react. Anti-OPTN antibody (Cat. No. 10837-1-AP) was purchased from ProteinTech Group, Inc. (Chicago, IL), and anti-NRL antibody (sc-10971) was purchased from Santa Cruz Biotechnology, Inc. (Santa Cruz, CA), both of which detect human proteins. Anti-NRL antibody cross-reacts with the rat counterpart of NRL (Nrl). We confirmed that the anti-OPTN antibody can be used for the rat counterpart of OPTN (Optn) by Western blot analysis, as also that the anti-NRL and the anti-OPTN antibodies do not cross-react. Goat anti-mouse IgG/HRP (P0447), goat anti-rabbit IgG/HRP (P0448), and rabbit anti-goat IgG/HRP (P0449) were purchased from DAKO (Tokyo, Japan). AlexaFluor488-donkey anti-goat IgG (A11055), AlexaFluor488-donkey anti-mouse IgG (A21202) and AlexaFluor594-donkey anti-rabbit IgG (A21207) were purchased from Invitrogen (Carlsbad, CA).

cDNA cloning

cDNA for the *NRL* and *OPTN* genes was amplified by polymerase chain reaction (PCR) with human retina marathon cDNA (TAKARA, Japan). The nucleotide sequences of *NRL* (Acc. No. NM_006177) and *OPTN* (NM_001008211) cDNA were obtained from RefSeq, NCBI (http://www.ncbi.nlm.nih.gov/). The open reading frame sizes were 714 and 1,734 bp for *NRL* and *OPTN*, respectively. PCR primers were designed from these sequences, and the recognition sites for restriction endonuclease *Hin*dIII and *Eco*RI for NRL and *Bsa*I and *Eco*RI for OPTN were introduced into each primer. The names and sequences of the PCR primers for *NRL* are as follows: NRL. *Hin*dIII.F, CCCAGCAagcttATGGCCCTGCCCCCCAG-CCCCCT; and NRL.*Eco*RI.R, GCTCTGgaattcTCAGAGGAA-GAGGTGGGAGGG. Those for *OPTN* are as follows: OPTN. *Bsa*I.F, TTCCACggtctcAAGCTTATGTCCCATCAACCTCT-CAG; and OPTN.*Eco*RI.R, ATACATgaattcTTAAATGATGC-AATCCATCA.

After PCR amplification, *NRL* cDNA was cut with *Hin*dIII and *Eco*RI and inserted into the *Hin*dIII and *Eco*RI sites of a 3 × HA vector (a gift of Drs. A. Takayanagi and N. Shimizu) (Lim et al., 2007). Similarly, *OPTN* cDNA was amplified, cut with *Bsa*I and *Eco*RI, and inserted into the *Hin*dIII and *Eco*RI sites of a p3 × FLAG-CMV-7.1 expression vector (Sigma–Aldrich). The PCR primer OPTN.BsaI.F was designed to obtain the same protruding sequence as that produced by *Hin*dIII when the amplified product was cut by *Bsa*I to enable a ligation reaction with the vector edge cut by *Hin*dIII. For NRL and OPTN cDNA mock experiments, we used YPEL5 cDNA (Hosono et al., 2010), which shares no homology to the sequences of NRL and OPTN and was not expected to interact with them. YPEL5 cDNA was inserted into the 3 × HA vector and p3 × FLAG-CMV-7.1 expression vector. The nucleotide sequences of all clones were confirmed as the same as the designed sequences.

Construction of a deletion series of OPTN-expression plasmids

A series of deletion OPTN plasmids was constructed using the KOD-Plus-Mutagenesis Kit (TOYOBO) with the following PCR primers: OPTN_Lc1st-R, AAGCTTGTCATCGT-CATCCTTGTAATC, and OPTN_Lc1st-F, TCATCTGAGG-ACCCCACTGATG for OPTNdel1st (1–120); OPTN_LcM-R, CCTTTCTGATTTCCCTTTTAG, and OPTN_LcM-F, GAA-GAGAAAGGCCCGGAGA for OPTNdel2nd (121–287); OPTN_Lc3rd-R, ATCATTCTCTTTCTCTGTGCT- CCC, and OPTN_Lc3rd-F, CTGAAGGAACTGAGTGAAAAACT-GGA for OPTNdel3rd (288–422) and OPTN_Lc4th-R, CAC-TGCCCTGTCCACTTTTTCTG, and OPTN_Lc4th-F, TAAG-AATTCATCGATAGATCTGATATCGG for OPTNdel4th (423–577).

Cell culture, DNA transfection and immunofluorescent staining

HeLaS3 cells were cultured on coverslips in Dulbecco's modified Eagle medium containing 10% foetal bovine serum under standard cell culture conditions. DNA transfection involved FuGENE6 (Roche, Indianapolis, IN). Briefly, the

cells were treated with FuGENE6 in the same serum-containing medium for 24 h. They were fixed in 4% paraformaldehyde after permeabilization by 0.5% Triton X-100 in phosphate buffered saline lacking Ca^{2+} and Mg^{2+}. Binding of the primary and secondary antibodies was done at room temperature for 1 h and 30 min, respectively. Fluorescent signals were observed using a fluorescence microscope [Axioskop-2plus (Zeiss, Goetingen, Germany)].

Proximity ligation assay

Cells cultured on coverslips were co-transfected with HA-NRL and FLAG-OPTN plasmids. After fixation and binding of the rabbit anti-HA and mouse anti-FLAG primary antibodies, cells were treated with secondary antibodies, that is, anti-rabbit Ig conjugated with a specific oligonucleotide (PLA probe MINUS) and anti-mouse Ig with another specific oligonucleotide (PLA probe PLUS). Next, Alexa-Fluor488-donkey anti-mouse IgG was applied to detect FLAG-OPTN, which was followed by PLA probe hybridisation, the ligation reaction to form closed circular DNA, amplification by the rolling circle reaction, and final hybridisation of the amplified DNA-specific fluorescent oligo DNA probe. PLA hybridisation signals were detected using a fluorescent microscope (Axioskop-2plus, Zeiss).

Cell fractionation

Cell fractionation was done in 50 mM Tris–HCl/0.15 M NaCl/1 mM EDTA (pH 7.4) (TBS) and 1% Triton X-100 in TBS (Triton-TBS). Protease inhibitor complete EDTA-free (Roche) cocktail was added to TBS and Triton-TBS. Cells were suspended in Triton-TBS for disruption to prepare the cell lysate. The whole cell lysate was centrifuged at 500*g* for 5 min and the supernatant used for immunoprecipitation. To prepare nuclear and cytoplasmic fractions, cells were mildly disrupted in hypotonic buffer (10 mM Tris–HCl, 10 mM KCl, 1.5 mM $MgCl_2$, 0.5 mM DTT, pH 7.9 and the protease inhibitor) using a homogeniser, and the undisrupted cells were removed by low-speed centrifugation. High-speed centrifugation (5000*g*, 10 min) was used to separate the cytoplasmic fraction (supernatant) and nuclei (precipitate). Nuclei were destroyed in hypertonic buffer (20 mM Tris–HCl, 420 mM NaCl, 1.5 mM $MgCl_2$, 0.5 mM DTT, 25% glycerol, pH 7.9 and the protease inhibitor), using an ultrasonic disruptor (Sonicator UD-201, TOMY, Tokyo, Japan) on ice at power level 2 for 20 s (50% duty cycle). The supernatant from the same high-speed centrifugation was used as the nuclear fraction.

Immunoprecipitation

Protein G Sepharose 4 Fast Flow (GE Healthcare, Piscataway, NJ) was equilibrated with Triton-TBS, and the appropriate antibody was added to the solution for $\geq$2 h. After washing in Triton-TBS, the whole-cell, cytoplasmic or nuclear lysate was added to allow antigen–antibody binding overnight. After the lysates had been washed with Triton-TBS, sample buffer for sodium dodecyl sulphate–polyacrylamide gel electrophoresis (SDS–PAGE) was added, and the samples were boiled. The supernatant was applied to an SDS–PAGE gel.

Western blotting

Proteins in the SDS–PAGE gel were electroblotted to Immobilon-P (MILLIPORE, Chelmsford, MA) membrane filters in a semi-dry apparatus at 1.2 mA/cm^2 for 60 min. Primary and HRP-labelled secondary antibodies were bound using a standard protocol, and 5% skim milk was used to block non-specific binding. Luminescent detection was performed using ImmunoStar Reagent (Wako, Tokyo, Japan), and the luminescent images were analysed by LAS1000 mini (Fuji Film, Tokyo, Japan).

Immunofluorescent staining of rat retina

Rats were handled in adherence to the ARVO statement for the use of animals in ophthalmic and vision research.

Ten-week old male Wistar rats, purchased from Japan SLC Co., Ltd. (Hamamatsu, Japan), were anaesthetised by ether inhalation, and perfused and fixed with 2% paraformaldehyde-containing 0.1 M phosphate buffer (pH 7.4) at 4°C. The eyes were enucleated and immersed in the same fixative for 10 min, and the cornea, lens and vitreous humour were removed to form an eyecup under a stereoscopic microscope. The eyecup was immersed in the fixative for 4 h at 4°C, cryoprotected sequentially in PBS(−) containing 15%, 20% and 25% sucrose at 4°C for 4 h each and promptly frozen in Tissue-Tek O.C.T. compound (Sakura Finetek USA, Inc., Torrance, CA, USA) in liquid nitrogen. The frozen block was sectioned in the sagittal plane using a cryostat (CM 1510-11, Leica Microsystems GmbH, Wetzlar, Germany; Finetec, Co. Ltd., Tokyo, Japan) to generate sections of 4 and 10 μm. The frozen sections were mounted onto MAS-coated slides (Matsunami Glass Ind., Ltd., Osaka, Japan) and dried using a handheld hair dryer for 1 h.

Immediately before use, the sections on slides were immersed in methanol at −25°C for 1 h and treated with 2% skim milk in PBS(−) for 2 h at room temperature to block non-specific binding of antibodies. They were incubated with rabbit anti-OPTN (1:100) and goat anti-NRL (1:50) antibodies in PBS(−) containing 1% bovine serum albumin (BSA) for 1 h at room temperature. After washing with PBS(−) three times for 5 min each, the sections were treated with 2% non-immune donkey serum in PBS(−) for further blocking. Incubation with the secondary antibodies AlexaFluor488-donkey anti-rabbit immunoglobulin

(IgG) (1:500) and AlexaFluor594 donkey anti-goat IgG (1:500) in PBS(−) containing 1% BSA was performed for 1 h at room temperature. After washing, nuclei were counterstained with 4′,6-diamidino-2-phenylindole (DAPI) (Invitrogen, Tokyo, Japan). The sections were mounted under a coverslip in Fluoromount medium (Diagnostic Biosystems, Pleasanton, CA, USA) and observed using a fluorescence microscope (Axioskop 2 plus; Carl Zeiss Co., Ltd., Tokyo, Japan). For negative staining, non-immune rabbit IgG and goat IgG (Novagen, Madison, WI, USA) were used instead of the primary antibody.

Results

Interaction of tagged NRL and OPTN in HeLaS3 cells

Coding regions of human NRL and OPTN cDNA were prepared by PCR, cloned into N-terminal-HA-tagged and N-terminal-FLAG-tagged vectors, respectively, and co-transfected into HeLaS3 cells. The expression and localisation of HA-tagged NRL (HA-NRL) and FLAG-tagged OPTN (FLAG-OPTN) in the cells were followed by double immunofluorescence staining using anti-tag antibodies. Anti-HA antibody stained the nuclei (Figure 1C), which is consistent with the localisation of NRL (Swain et al., 2001). In contrast, anti-FLAG antibody staining was found not only in the cytoplasm, but in the nucleus (Figure 1D). The staining signal in the nucleus was weaker than in the cytoplasm, but still appeared non-artifactual, which suggests that a small amount of FLAG-OPTN is localised to the nucleus. The intensity of the FLAG-OPTN (green) signal in the nucleus varied among cells, and nuclei with a stronger signal showed more yellow colour mixed with the HA-NRL (red) signal (Figure 1A). The staining profile of FLAG-OPTN in the cytoplasm was fairly even, probably because of overexpression. Therefore, we transfected cells with only the HA-NRL plasmid (Figures 1E–1H). Endogenous OPTN was detected using its specific antibody (Figure 1H). The signal intensity was generally lower than that of FLAG-OPTN, but the Golgi apparatus staining near the nucleus was seen as previously reported (Rezaie et al., 2002). In this case, the anti-OPTN signal in the nuclei was also clear, although it was weaker than in the cytoplasm (Figure 1H), which suggests that OPTN is at least partially localised to the nuclei.

We examined the interaction between HA-NRL and FLAG-OPTN co-expressed in HeLaS3 cells in two ways. First, we immunoprecipitated it for Western blot analysis (IP-WB analysis) to determine whether NRL and OPTN might be co-immunoprecipitated. Second, we did a proximity ligation assay (PLA). For IP-WB analysis, plasmid cDNA encoding HA-NRL and FLAG-OPTN was co-transfected into HeLaS3 cells, and whole cell lysates were prepared using Triton-TBS, with the negative controls being plasmids containing the coding sequence of an unrelated protein; YPEL5 (HA-YPEL5 or FLAG-YPEL5) were used rather than HA-NRL or FLAG-OPTN. Following immunoprecipitation with the anti-FLAG antibody, the immunoprecipitate was detected by Western blotting using anti-HA antibody, and a 33-kDa band corresponding to the size of NRL (29 kDa) with the HA-tag (4 kDa) (left lane of the upper panel in Figure 2A) was found. Immunoprecipitation with the anti-HA antibody gave a 75-kDa band with anti-FLAG antibody (left lane of lower panel in Figure 2C). Although the calculated size of FLAG-OPTN is 69 kb (66 kDa of OPTN plus the 3-kDa FLAG-tag), the 75-kDa band was considered to be FLAG-OPTN because this apparently larger size of FLAG-OPTN in SDS–PAGE was seen previously (Park et al., 2006, 2010). Mock transfection with plasmids expressing YPEL5 cDNA did not produce

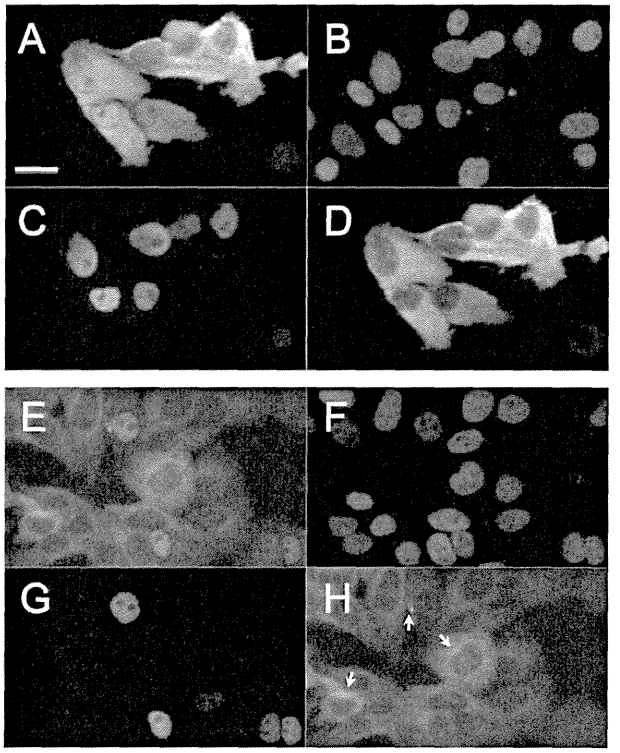

Figure 1 Immunofluorescence staining of HeLaS3 cells using anti-HA and anti-FLAG or anti-OPTN. HeLaS3 cells were transfected with HA-NRL and FLAG-OPTN plasmids (A–D) or with HA-NRL plasmid only (E–H). (A–D) Cells were stained with anti-HA antibody (red) and anti-FLAG antibody (green). (A) Merged image of (C) and (D); (B) DAPI staining of nuclei; (C) staining with anti-HA antibody; (D) staining with anti-FLAG antibody. (E–H) Cells were stained with anti-HA antibody (red) and anti-OPTN antibody (green). (E) merged image of (G) and (H); (F) DAPI staining of nuclei; (G) staining with anti-HA antibody; (H) staining with anti-OPTN antibody. Arrows in (H) show Golgi-apparatus-like staining near the nuclei. Scale bar is 20 μm. Only cells in which plasmids were successfully transfected showed immunofluorescent signals (C, D and G). FLAG-OPTN signals in nuclei were weaker than those in the cytoplasm, but still non-artifactual (D and H).

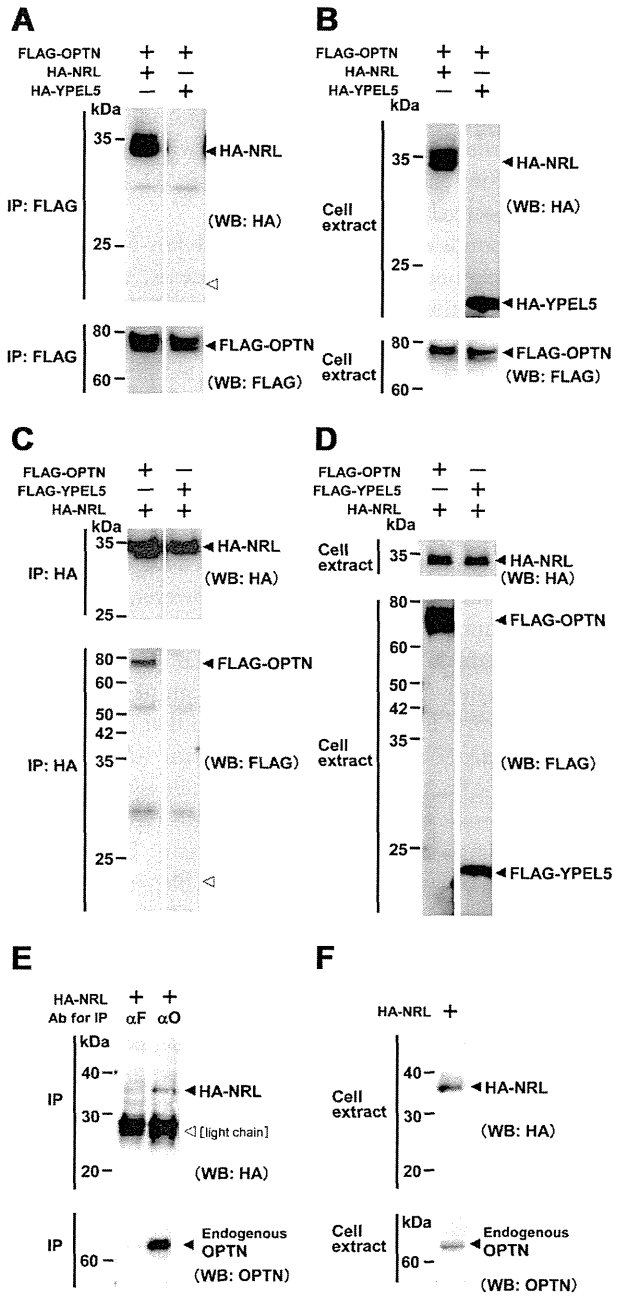

Figure 2 Co-immunoprecipitation of HA-NRL and FLAG-OPTN expressed in HeLaS3 cells. (A) Immunoprecipitation performed with the anti-FLAG antibody. The presence of transfected plasmid DNA is indicated at the top by plus (+) and minus (–). Western blotting was used with the anti-HA antibody (upper panel) and the anti-FLAG antibody (lower panel). The open arrowhead shows the position around 22–23 kDa corresponding to the size of HA-YPEL5. (B) Western blot analysis of input proteins used for the immunoprecipitation shown in (A). The presence of transfected plasmid DNA is indicated at the top by plus (+) and minus (–). Western blotting was used with the anti-HA antibody (upper panel) and anti-FLAG antibody (lower panel). (C) Immunoprecipitation performed with the anti-HA antibody. The presence of transfected plasmid DNA is indicated at the top by plus (+) and minus (–). Western blotting was used with the anti-HA antibody (upper panel) and the anti-FLAG antibody (lower panel). The open arrowhead shows the position around 22–23 kDa corresponding to the size of HA-YPEL5. (D) Western blot analysis of input proteins used for the immunoprecipitation shown in (C). The presence of transfected plasmid DNA is indicated at the top by plus (+) and minus (–). Western blotting was used with the anti-HA antibody (upper panel) and anti-FLAG antibody (lower panel). (E) Immunoprecipitation performed with the anti-FLAG or anti-OPTN antibody. Antibodies (Ab) used for immunoprecipitation in the left and right lanes are anti-FLAG (αF) and anti-OPTN (αO), respectively. Western blotting was used with the anti-HA antibody (upper panel) and the anti-OPTN antibody (lower panel). The thick band shown with an open arrowhead is the light chain of the antibody. (F) Western blot analysis of input proteins used for immunoprecipitation shown in (E). Western blotting was done with the anti-HA antibody (upper panel) and anti-OPTN antibody (lower panel). IP, immunoprecipitation; WB, Western blotting.

bands at the corresponding size of 22–23 kDa (open arrowheads shown in right lanes of the upper panel in Figure 2A and the lower panel in Figure 2C). Cell extracts without immunoprecipitation were directly assayed, and the respective tagged proteins were found (Figures 2B and 2D), confirming the presence of tagged proteins in cell lysates. These results show that the HA-tagged NRL and FLAG-tagged OPTN proteins were co-immunoprecipitated and suggest that these two proteins interact when co-expressed in HeLaS3 cells.

IP-WB analysis was used for cells transfected with only the HA-NRL plasmid to assay the interaction between HA-NRL and endogenous OPTN. Cell lysate was prepared and used for immunoprecipitation with an anti-OPTN antibody, and the immunoprecipitate was probed with anti-HA antibody. A 66-kb band (right lane of the lower panel in Figure 2E) was considered to be endogenous OPTN. Thus, HA-NRL was co-immunoprecipitated with endogenous OPTN, which indicates interaction between OPTN and NRL.

To confirm that FLAG-OPTN and HA-NRL interact with each other intracellularly, PLA analysis was used. HeLaS3 cells were co-transfected with HA-NRL and FLAG-OPTN plasmids. Strong PLA signals were seen in cell nuclei (Figures 3D and 3H). Because DNA amplification in PLA occurs only when two proteins exist in close proximity, this finding indicates that HA-NRL and FLAG-OPTN interacted with each other in the nucleus, ruling out the possibility of their interacted during preparation of the lysate.

Determination of the region of OPTN necessary for NRL binding

A set of plasmids was constructed with different partial deletions of the OPTN-coding sequence (Figure 4) to determine the region of OPTN necessary for NRL binding. The boundaries of these deletions were decided according to a previously reported homology analysis with NEMO

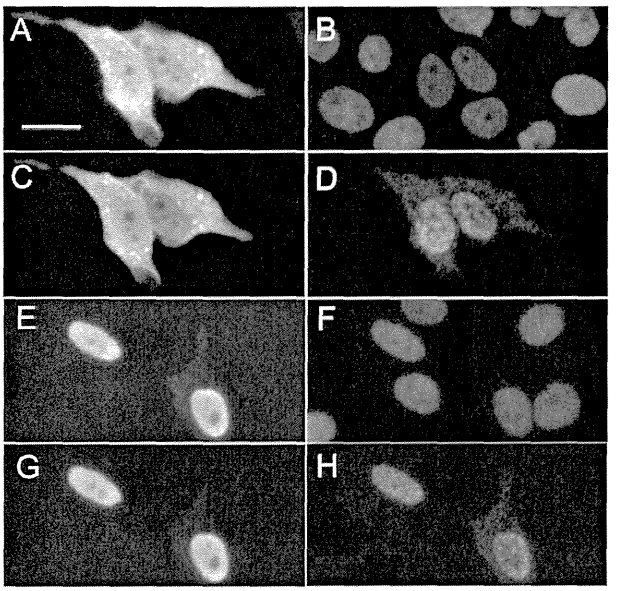

Figure 3 Detection of probable binding between FLAG-OPTN and HA-NRL using the proximity ligation assay in HeLaS3 cells. (A–D) and (E–H) are the same views. (A) Merged image of (C) and (D). (E) Merged image of (G) and (H). (B and F) DAPI staining of nuclei. (C) Staining with anti-FLAG antibody detected by fluorescent secondary antibody (Alexa-Fluor488-donkey anti-mouse IgG). (G) Staining with anti-HA antibody detected by fluorescent secondary antibody (AlexaFluor594-donkey anti-mouse IgG). (D and H) Signals from proximity ligation assay (PLA) using anti-FLAG and anti-HA antibodies. Scale bar is 20 μm. Only cells in which plasmids were successfully transfected showed immunofluorescent signals (C and G). Strong PLA signals were detected in the nuclei (D and H).

(Schwamborn et al., 2000). The tail region (423–577 aa) with the highest NEMO homology; the left middle region (121–287 aa), which does not have a corresponding region in NEMO; and the first and third regions (1–120 and 288–422 aa, respectively) with low NEMO homology were selected for deletion (see the plasmid constructs in Figure 4). The corresponding deletion clones were named del1st, del2nd, del3rd and del4th in order of their position in OPTN. The calculated protein sizes for partial OPTN with the FLAG tag expressed from these four plasmids were 55, 50, 53 and 51 kDa, respectively.

These plasmids were co-transfected with HA-NRL. For the following immunoprecipitation experiments, cytoplasmic and nuclear fractions were used rather than whole cell lysates to analyse the protein localisation in greater detail. Immunoprecipitation used anti-FLAG antibody for the cytoplasmic and nuclear fractions of cells transfected with one of the four deletions OPTN plasmids, followed by Western blot analysis with anti-HA-tag antibody (Figure 5A, lanes 3–6). In the nuclear fractions of cells transfected with the del1st, del2nd or del3rd plasmid, a band of co-immunoprecipitated HA-NRL was detected (arrows in lanes 3Nu, 4Nu and 5Nu in Figure 5A). However, the del4th plasmid did not produce a band (Figure 5A, lane 6Nu), which suggests that the NRL-binding region of OPTN is located in the fourth region (Figure 4). A higher-brightness picture of lane 6Nu (lane 6′ in Figure 5A) confirmed that there was no band in the HA-NRL position. The NRL band was not found in cytoplasmic fractions from cells transfected with any of the deletion plasmids or with the whole-length OPTN plasmid (Figure 5A, lanes 3–6Cy and 1Cy). The same immunoblot used in Figure 5A was analysed by Western blotting with anti-FLAG antibody (Figure 5B). Bands sized 63 kDa (lanes 3Cy and 3Nu), 55 kDa (4Cy and 4Nu), 60 kDa (5Cy and 5Nu) and 58 kDa (6Cy and 6Nu) were detected in the cytoplasmic and nuclear fractions (bracket in Figure 5B), which appear to correspond to FLAG-OPTN with partial deletions. All these apparent sizes were greater than the calculated sizes, which is

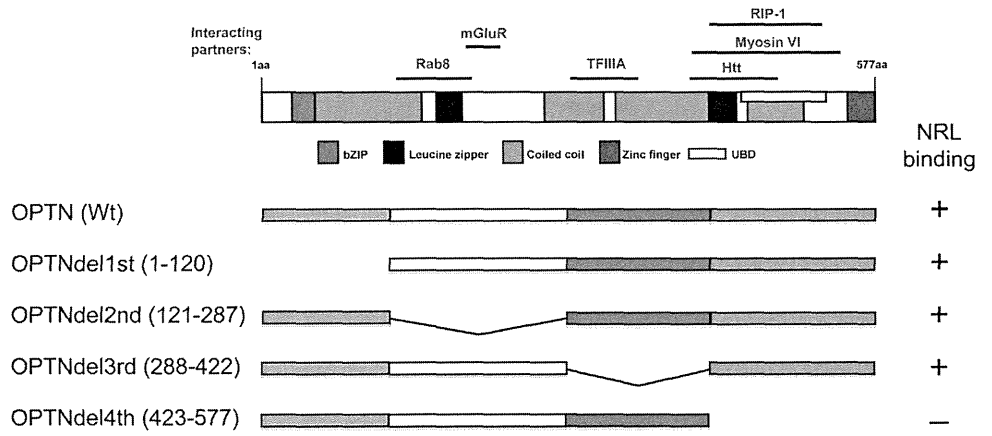

Figure 4 Construction of partial-deletion OPTN plasmids. The four deleted regions are shown. The top part of this figure was compiled from a previous report (Chalasani et al., 2009) with several modifications. bZIP, Leucine zipper, Coiled coil, Zinc finger and UBD represent the functional domains of OPTN. Horizontal bars show the binding regions of various proteins. The ability of NRL to bind each of the partial-deletion OPTN proteins from these plasmids in the assay described in Figure 5 is indicated by a plus or minus sign.

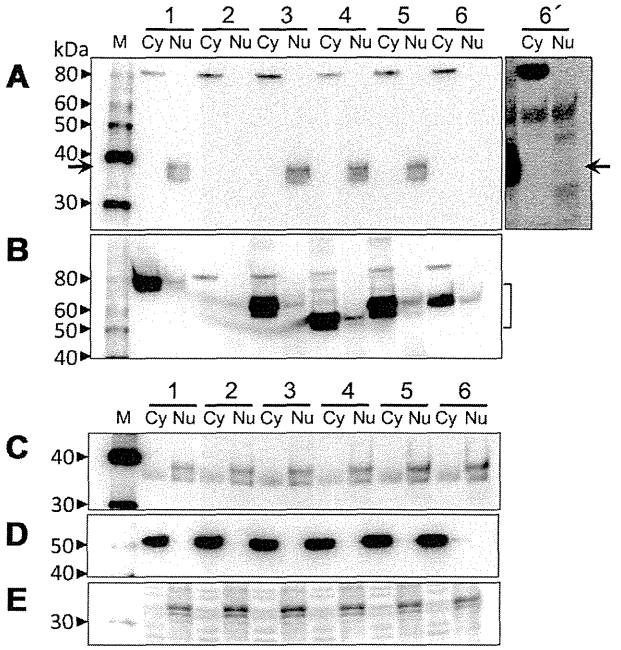

Figure 5 Determination of the OPTN region necessary for NRL binding. (A) Western blot analysis using the anti-HA antibody on immunoprecipitates obtained with the anti-FLAG antibody from the cytoplasmic (Cy) and nuclear (Nu) fractions after transfection with a series of partial deletion FLAG-OPTNs together with the HA-NRL plasmid. The arrow indicates the position of HA-NRL. (B) Western blot analysis using the anti-FLAG antibody in the same blot shown in (A). The bracket shows the band positions of partial-deletion FLAG-OPTN proteins. (C) Western blot analysis of all fractions without immunoprecipitation using the anti-HA antibody. (D) Western blot analysis of all fractions without immunoprecipitation using the anti-alpha-tubulin antibody. (E) Western blot analysis of all fractions without immunoprecipitation using the anti-histone H1 antibody. In Lanes 1–6, the following plasmids were used for transfection: Lane 1, full-length FLAG-OPTN; Lane 2, no plasmids; Lane 3, OPTNdel1st (1–120); Lane 4, OPTNdel2nd (121–287); Lane 5, OPTNdel3rd (288–422); and Lane 6, OPTNdel4th (423–577). Arrows in (A) show the position of HA-NRL. Lane 6′ shows the same blot as Lane 6 but with longer exposure time for signal detection, in which no specific HA-NRL band appeared. The bands seen in Lanes 1–6 Cy in (A) are non-specific. M stands for the molecular weight markers.

similar to the case for full-length FLAG-OPTN described above. The amount of full-length or deletion FLAG-OPTN found in nuclear fractions was much lower than that in the cytoplasm, but was clearly non-artifactual (Figure 5B, lanes 1, 3–6Nu). This finding indicates that a small amount of nuclear-localised FLAG-OPTN, with the exception of del4th, bound to HA-NRL. Western blot analysis of all fractions without immunoprecipitation using the anti-HA antibody also detected HA-NRL bands with modest intensity in the cytoplasm fractions (Figure 5C), which indicates that HA-NRL was present in the cytoplasmic fractions, but did not bind to FLAG-OPTN. The amount of alpha-tubulin and histone H1, marker proteins for the cytoplasm and nuclear fractions, respectively, was analysed to detect contamination of the nuclear fraction by cytoplasmic components or vice versa, but no significant contamination was detected (Figures 5D and 5E). These results show that FLAG-OPTN binds to HA-NRL in the nucleus and that the NRL-binding region of OPTN is located in its tail region (423–577 aa).

Expression and localisation of Optn and Nrl in the rat retina

To investigate the localisation of rat homologues of OPTN and NRL (Optn and Nrl) in the rat retina, we immunostained rat retinal sections with anti-OPTN and anti-NRL antibodies, for which cross-reactivity to rat Nrl and Optn had been confirmed. Strong fluorescent signals from the anti-OPTN antibody were seen in the outer plexiform layer (OPL), the outer nuclear layer (ONL) and the inner segments of the photoreceptors (IS) (Figures 6A and 6B). Medium-intensity signals were detected in ganglion cells, and weaker but clear signals were also detected in the inner plexiform and inner nuclear layer (IPL and INL). Anti-NRL immunoreactivity was seen in the ONL and IS (Figure 6D). High-power images of ONL for anti-OPTN staining showed fluorescent signals in the cytoplasm of most photoreceptor cells (Figure 6G). However, the nuclei of these cells did not show anti-OPTN staining even though they were stained with the anti-NRL antibody (Figures 6G, 6I and 6J). These results indicate that Optn is expressed in rat photoreceptor cells, and is localised in the cytoplasm, but no detectably in the nucleus.

Discussion

Having shown co-immunoprecipitation of FLAG-OPTN and HA-NRL that had been co-transfected in HeLaS3 cells, and that endogenous OPTN co-immunoprecipitated with HA-NRL with close proximity of FLAG-OPTN and HA-NRL in the nucleus with close proximity, it seems that OPTN and NRL interact in the nuclei. Various OPTN-binding proteins have been reported, including huntingtin, TFIIIA, Rab8 and myosin VI (Chalasani et al., 2008), all of which are expressed in the eyes and various other tissues. However, NRL is a rod-specific protein (Swain et al., 2001), and is the first OPTN-binding protein identified to have eye-specific expression. NRL-binding region of OPTN is limited to the tail portion (423–577 aa), which contains binding regions for other proteins, including RIP-1, myosin VI and huntingtin (Figure 4). This information will be useful in analysing the interaction between OPTN and NRL. We have also shown OPTN expression in photoreceptor cells, which seems to be a novel finding.

Since the first report on NRL (Swaroop et al., 1992), many studies have considered its relevance in ocular diseases. NRL and its animal homologue control the differentiation of rods from their progenitor cells during eye morphogenesis and regulate the expression of various rod-specific genes, such as

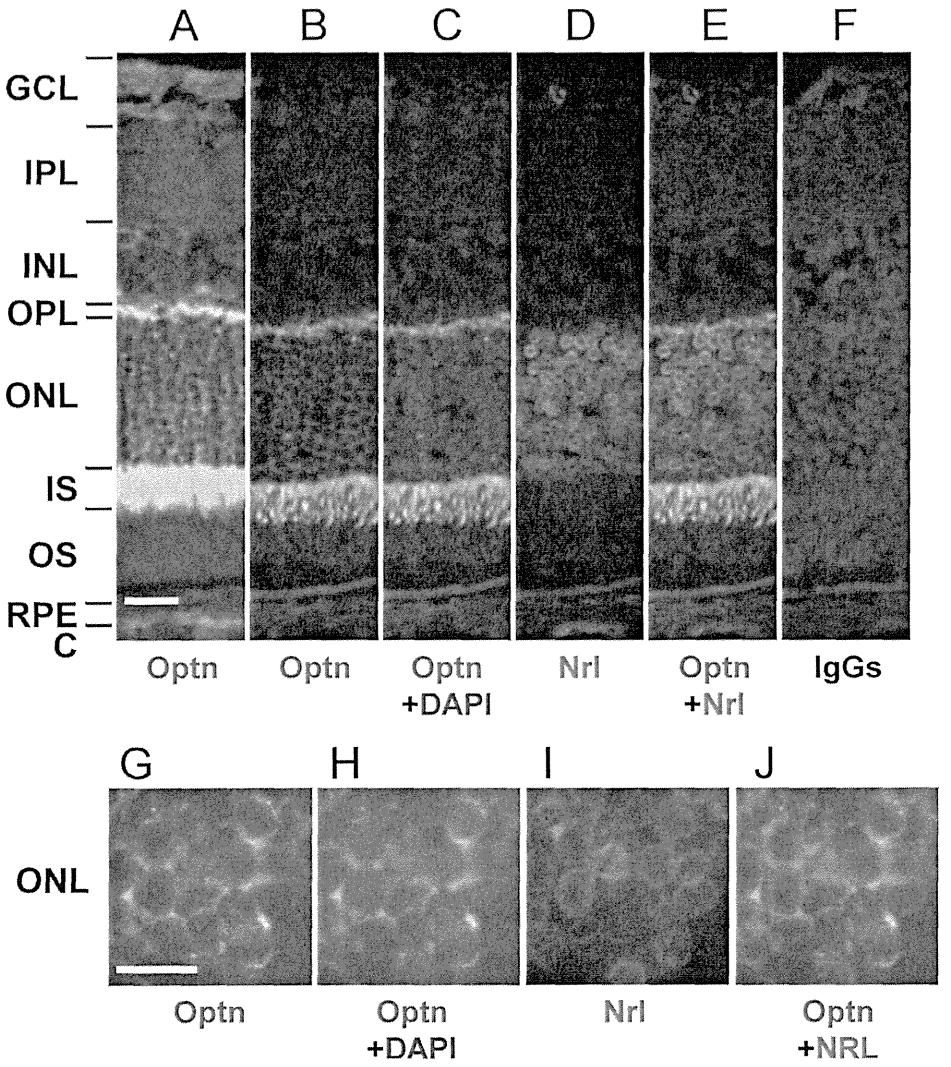

Figure 6 Expression of Optn in rat photoreceptor cells. Sections of rat retina were stained with anti-OPTN and anti-NRL antibodies. (A, B and G) Fluorescent images with anti-OPTN antibody. (D and I) Fluorescent images with anti-NRL antibody. (E and J) Merged images of (A and D) and (G and I), respectively. (C and H) Merged images of (B) or (G) with DAPI counterstaining, respectively. (F) A negative control image using non-immunised IgG to show no significant signals of anti-OPTN and anti-NRL antibodies. (B–E) are images of the same field. (B–E) are images of the same field at positions similar to those of (A–F) under high power. The thickness of the sections was 10 μm in (A) and 4 μm in (B–J). The scale bar is 20 μm in (A–F) and 10 μm in (G–J). GCL, ganglion cell layer; IPL, inner plexiform layer; INL, inner nuclear layer; OPL, outer plexiform layer; ONL, outer nuclear layer; IS, inner segment. The doughnut-ring-like staining of nuclei with the anti-NRL antibody was reproducible, and similar staining of Nr2e3 and Otx2 proteins in mouse photoreceptor nuclei was previously reported (Chen et al., 2005; Fossat et al., 2007).

rhodopsin, in adults (Kumar et al., 1996; Rehemtulla et al., 1996; Oh et al., 2007). Mutations in the NRL gene cause RP (Bessant et al., 1999). Thus, the characteristics of NRL as a transcriptional regulator and an RP-causing factor are well documented. However, the interaction of NRL with OPTN, which causes glaucoma, remains unclear.

OPTN partially relocates from the cytoplasm to the nucleus in a Rab8-dependent manner under stressed conditions, such as H_2O_2 exposure (De Marco et al., 2006). We have shown that a small amount of endogenous OPTN and FLAG-OPTN localises in the nucleus of HeLaS3 cells in the absence of stress. However, Optn was not detected in the nuclei of rat photoreceptor cells, and therefore it is possible that Optn in rat photoreceptors is relocated to the nucleus under some type of stress. Detailed analyses of OPTN localisation and possible interaction with NRL in photoreceptor cells are necessary to elucidate the significance of the binding of OPTN with NRL.

Acknowledgements and funding

The authors thank Dr. A. Takayanagi (Department of Molecular Biology, Keio University School of Medicine,

Tokyo, Japan) and Prof. Emeritus N. Shimizu (Advanced Research Center for Genome Super Power, Keio University, Tsukuba, Japan) for providing the 3 × HA vector, Mr. Katsuhisa Ishii for his persistent efforts to obtain PLA signals in a lab course, and Prof. Duco Hamasaki (Bascom Palmer Eye Institute, University of Miami School of Medicine, Miami, FL) for his helpful comments and editorial support in manuscript preparation. This study was supported in part by a Grant-in-Aid for Scientific Research on Priority Areas from the Ministry of Education, Culture, Sports, Science and Technology (MEXT) and a Grant-in-Aid for Scientific Research from the Japan Society for the Promotion of Science (JSPS). Chunxia Wang is the scholarship student of the Japanese Government (Monbukagakusho: MEXT) (2003–2008); 2009 Santen Pharmaceutical Travel Grant from the Association for Research in Vision and Ophthalmology (ARVO).

References

Bessant DA, Payne AM, Mitton KP, Wang QL, Swain PK, Plant C, Bird AC, Zack DJ, Swaroop A, Bhattacharya SS (1999) A mutation in NRL is associated with autosomal dominant retinitis pigmentosa. Nat Genet 21: 355–6.

Chalasani ML, Radha V, Gupta V, Agarwal N, Balasubramanian D, Swarup G (2007) A glaucoma-associated mutant of optineurin selectively induces death of retinal ganglion cells which is inhibited by antioxidants. Invest Ophthalmol Vis Sci 48: 1607–14.

Chalasani ML, Balasubramanian D, Swarup G (2008) Focus on molecules: optineurin. Exp Eye Res 87: 1–2.

Chalasani ML, Swarup G, Balasubramanian D (2009) Optineurin and its mutants: molecules associated with some forms of glaucoma. Ophthalmic Res 42: 176–84.

Chen J, Rattner A, Nathans J (2005) The Rod photoreceptor-specific nuclear receptor Nr2e3 represses transcription of multiple cone-specific genes. J Neurosci 25: 118–29.

De Marco N, Buono M, Troise F, Diez-Roux G (2006) Optineurin increases cell survival and translocates to the nucleus in a Rab8-dependent manner upon an apoptotic stimulus. J Biol Chem 281: 16147–56.

Faber PW, Barnes GT, Srinidhi J, Chen J, Gusella JF, MacDonald ME (1998) Huntingtin interacts with a family of WW domain proteins. Hum Mol Genet 7: 1463–74.

Fossat N, Le Greneur C, Béby F, Vincent S, Godement P, Chatelain G, Lamonerie T (2007) A new GFP-tagged line reveals unexpected Otx2 protein localization in retinal photoreceptors. BMC Dev Biol 7: 122.

Hosono K, Noda S, Shimizu A, Nakanishi N, Ohtsubo M, Shimizu N, Minoshima S (2010) YPEL5 protein of the YPEL gene family is involved in the cell cycle progression by interacting with two distinct proteins RanBPM and RanBP10. Genomics 96: 102–11.

Kroeber M, Ohlmann A, Russell P, Tamm ER (2006) Transgenic studies on the role of optineurin in the mouse eye. Exp Eye Res 82: 1075–85.

Kumar R, Chen S, Scheurer D, Wang QL, Duh E, Sung CH, Rehemtulla A, Swaroop A, Adler R, Zack DJ (1996) The bZIP transcription factor Nrl stimulates rhodopsin promoter activity in primary retinal cell cultures. J Biol Chem 271: 29612–8.

Li Y, Kang J, Horwitz MS (1998) Interaction of an adenovirus E3 14.7-kilodalton protein with a novel tumor necrosis factor alpha-inducible cellular protein containing leucine zipper domains. Mol Cell Biol 18: 1601–10.

Lim MK, Kawamura T, Ohsawa Y, Ohtsubo M, Asakawa S, Takayanagi A, Shimizu N (2007) Parkin interacts with LIM kinase 1 and reduces its cofilin-phosphorylation activity via ubiquitination. Exp Cell Res 313: 2858–74.

Maruyama H, Morino H, Ito H, Izumi Y, Kato H, Watanabe Y, Kinoshita Y, Kamada M, Nodera H, Suzuki H, Komure O, Matsuura S, Kobatake K, Morimoto N, Abe K, Suzuki N, Aoki M, Kawata A, Hirai T, Kato T, Ogasawara K, Hirano A, Takumi T, Kusaka H, Hagiwara K, Kaji R, Kawakami H (2010) Mutations of optineurin in amyotrophic lateral sclerosis. Nature 465: 223–6.

Mears AJ, Kondo M, Swain PK, Takada Y, Bush RA, Saunders TL, Sieving PA, Swaroop A (2001) Nrl is required for rod photoreceptor development. Nat Genet 29: 447–52.

Moreland RJ, Dresser ME, Rodgers JS, Roe BA, Conaway JW, Conaway RC, Hanas JS (2000) Identification of a transcription factor IIIA-interacting protein. Nucleic Acids Res 28: 1986–93.

Oh EC, Khan N, Novelli E, Khanna H, Strettoi E, Swaroop A (2007) Transformation of cone precursors to functional rod photoreceptors by bZIP transcription factor NRL. Proc Natl Acad Sci USA 104: 1679–84.

Park BC, Shen X, Samaraweera M, Yue BY (2006) Studies of optineurin, a glaucoma gene: Golgi fragmentation and cell death from overexpression of wild-type and mutant optineurin in two ocular cell types. Am J Pathol 169: 1976–89.

Park B, Ying H, Shen X, Park JS, Qiu Y, Shyam R, Yue BY (2010) Impairment of protein trafficking upon overexpression and mutation of optineurin. PLoS ONE 5: e11547.

Rehemtulla A, Warwar R, Kumar R, Ji X, Zack DJ, Swaroop A (1996) The basic motif-leucine zipper transcription factor Nrl can positively regulate rhodopsin gene expression. Proc Natl Acad Sci USA 93: 191–5.

Rezaie T, Sarfarazi M (2005) Molecular cloning, genomic structure, and protein characterization of mouse optineurin. Genomics 85: 131–8.

Rezaie T, Child A, Hitchings R, Brice G, Miller L, Coca-Prados M, Héon E, Krupin T, Ritch R, Kreutzer D, Crick RP, Sarfarazi M (2002) Adult-onset primary open-angle glaucoma caused by mutations in optineurin. Science 295: 1077–9.

Rezaie T, Waitzman DM, Seeman JL, Kaufman PL, Sarfarazi M (2005) Molecular cloning and expression profiling of optineurin

in the rhesus monkey. Invest Ophthalmol Vis Sci 46: 2404–10.

Schwamborn K, Weil R, Courtois G, Whiteside ST, Israël A (2000) Phorbol esters and cytokines regulate the expression of the NEMO-related protein, a molecule involved in a NF-kappa B-independent pathway. J Biol Chem 275: 22780–9.

Swain PK, Hicks D, Mears AJ, Apel IJ, Smith JE, John SK, Hendrickson A, Milam AH, Swaroop A (2001) Multiple phosphorylated isoforms of NRL are expressed in rod photoreceptors. J Biol Chem 276: 36824–30.

Swaroop A, Xu JZ, Pawar H, Jackson A, Skolnick C, Agarwal N (1992) A conserved retina-specific gene encodes a basic motif/leucine zipper domain. Proc Natl Acad Sci USA 89: 266–70.

Received 30 January 2013; accepted 22 July 2013.
Final version published online 12 September 2013.

Review article

http://dx.doi.org/10.6065/apem.2014.19.3.117
Ann Pediatr Endocrinol Metab 2014;19:117-121

Annals of Pediatric Endocrinology & Metabolism
apem

Neonatal screening and a new cause of congenital central hypothyroidism

Toshihiro Tajima, MD, PhD,
Akie Nakamura, MD,
Shuntaro Morikawa, MD,
Katsura Ishizu, MD

Department of Pediatrics, Hokkaido University School of Medicine, Sapporo, Japan

Congenital central hypothyroidism (C-CH) is a rare disease in which thyroid hormone deficiency is caused by insufficient thyrotropin (TSH) stimulation of a normally-located thyroid gland. Most patients with C-CH have low free thyroxine levels and inappropriately low or normal TSH levels, although a few have slightly elevated TSH levels. Autosomal recessive TSH deficiency and thyrotropin-releasing hormone receptor-inactivating mutations are known to be genetic causes of C-CH presenting in the absence of other syndromes. Recently, deficiency of the immunoglobulin superfamily member 1 (IGSF1) has also been demonstrated to cause C-CH. IGSF1 is a plasma membrane glycoprotein highly expressed in the pituitary. Its physiological role in humans remains unknown. IGSF1 deficiency causes TSH deficiency, leading to hypothyroidism. In addition, approximately 60% of patients also suffer a prolactin deficiency. Moreover, macroorchidism and delayed puberty are characteristic features. Thus, although the precise pathophysiology of IGSF1 deficiency is not established, IGSF1 is considered to be a new factor controlling growth and puberty in children.

Keywords: Congenital hypothyroidism (CH), Neonatal screening, Thyrotropin (TSH), IGSF1

Introduction

Congenital central hypothyroidism (C-CH) is an unusual condition characterized by low levels of both thyroid hormones and of thyroid-stimulating hormone (TSH). Patients with this disorder cannot be identified by neonatal screening programs based on TSH measurements[1,2]. However, neonatal screening for CH on the basis of thyroxine (T4) or free T4 and TSH concentrations can be performed to diagnose this type of CH[1-6].

C-CH is caused by mutations of transcription factors involved in pituitary development and differentiation, including *POU1F*, *PROP1*, *HESX1*, *LHX3*, and *LHX4*[7-9]. Because more than one pituitary cell type is deficient in these genetic diseases, patients with mutations of transcription factors often present with as a multiple pituitary hormone deficiency[7-9]. On the other hand, C-CH presenting in the absence of other syndromes remains a rare disease and is due mainly to a genetic deficit of the β-subunit of TSH (OMIM 188540)[10,11] or mutations of the thyrotropin-releasing hormone (TRH) receptor (OMIM 188545)[12,13]. Recently, it has been demonstrated that deficiency of immunoglobulin superfamily member 1 (IGSF1) (OMIM 300888) can also be a cause of C-CH[14-17]. This review will focus on clinical findings in patients with mutations of *IGSF1*, and the molecular basis of their disease.

Immunoglobulin superfamily member 1

IGSF1 is a plasma membrane immunoglobulin superfamily glycoprotein[18,19]. This protein has a putative signal peptide and twelve C2 type immunoglobulin (Ig)-like domain loops, a transmembrane domain, and a short intracellular C tail[19] (Fig. 1). The protein is

Received: 3 August, 2014
Accepted: 14 August, 2014

Address for correspondence:
Toshihiro Tajima, MD, PhD
Department of Pediatrics, Hokkaido University School of Medicine, N15, W7, Kita-Ku, Sapporo 060-8638, Japan
Tel: +81-11-716-1161
Fax: +81-11-706-7898
E-mail: tajeari@med.hokudai.ac.jp

ISSN: 2287-1012(Print)
ISSN: 2287-1292(Online)

cotranslationally cleaved such that only the C-terminal domain, containing 7 Ig loops, reaches the plasma membrane[19]. The gene encoding IGSF1 is located on Xq 26.2[18]. Human IGSF1 and murine *Igsf1* mRNAs are highly expressed in Rathke's pouch and in adult pituitary gland and testis[14]. Moreover, *IGSF1* protein is expressed in murine thyrotropes, somatotropes, and lactotropes, but not in gonadotropes or in the testis[14].

IGSF1 was initially hypothesized to be a candidate for the inhibin coreceptor in the pituitary gland, and it was therefore designated inhibin binding protein or p120.5[20]. However, *Igsf1* knockout mice showed no alternation of follicle stimulating hormone synthesis or secretion, and normal fertility[21]. Moreover, a recent *in vitro* study did not demonstrate binding of inhibin and IGSF1[22]. Thus, the physiological function of IGSF1 remains unknown.

Members of the IgSF have a wide variety of functions, acting as cell surface antigen receptors, coreceptors and costimulatory molecules of the immune system, molecules involved in antigen presentation to lymphocytes, cell adhesion molecules, certain cytokine receptors, and intracellular muscle proteins[23-28]. Some IgSF members play crucial roles not only in nervous system development but also in the adult during neural repair and synaptic plasticity[26-28]. Considering the function of other IgSF family members, IGSF1 may also act as a signal transduction molecule and/or cell adhesion molecule in the pituitary.

Neonatal screening for C-CH in Japan

In Sapporo city, the neonatal screening program for congenital hypothyroidism has employed the measurement of free T4 and TSH in the same filter-paper blood spot since 1986. This system has enabled us to identify C-CH in the neonatal period. Between January 2000 and December 2004, 83,232 newborns were screened and six C-CH patients identified as a result of follow-up of low free T4 and nonelevated TSH screening test results (a frequency of one in 13,872)[4]. Clinical characteristics and neonatal screening data of these patients are summarized in Table 1. Four showed multiple pituitary hormone deficiencies with pituitary malformations on magnetic resonance imaging. One patient was diagnosed as having Prader-Willie syndrome. Of these 6, the C-CH of a single one was caused by IGSF1 deficiency.

Adachi et al.[6] have recently reported the prevalence of C-CH in Kanagawa prefecture between 1999 and 2008. According to their study, neonatal screening for free thyroxine and TSH identified 24 C-CH patients, 14 of whom had multiple pituitary hormone deficiencies, eight had isolated C-CH, and two had undetermined pituitary involvement. Thus, the prevalence of CH-C was estimated at 1 in 30, 833 live births. During this period, 213 patients with CH of thyroid origin were diagnosed. Thus, C-CH constituted 10% of permanent CH detected by neonatal screening.

Lanting et al.[3] have reported the results of a neonatal screening program based on initial T4 and subsequent TSH determination with a T4 binding globulin in the Netherlands. In their study, among 385,000 infants screened during the period 1995–2000, the incidence of C-CH was 1:16,404 with 75% of C-CH diagnosed as having multiple pituitary hormone deficiency. This suggests that the incidence of isolated C-CH is likely to be around 1:65,000. Moreover, Joustra et al.[17] reported an IGSF1 defect in 8 of 11patients with isolated C-CH. Therefore, it is postulated that the incidence of C-CH caused by IGSF1 deficiency is approximately 1:100,000.

As mentioned above, in our small study over the short period 2004 to 2008, only one patient had a IGSF1 deficiency[4]. Thus, the incidence of IGSF1 deficiency was 1 in 80,000, but the exact prevalence of C-CH caused by IGSF1 deficiency in Japan cannot be said to have been determined. Further study is required.

Phenotypes associated with IGSF1 deficiency

In a previous report, six familial cases of C-CH in the Netherlands and one in Italy were identified by neonatal screening[14]. We have identified three *IGSF1*-deficient patients by neonatal screening[15,16]. ^{123}I scintigraphy showed a normal-sized thyroid in our patients. The Dutch study also showed normal-sized thyroids by ultrasound, except in one case[14].

In our study, one patient who was not identified by TSH screening in the neonatal period suffered growth retardation, and here, medical examination led to the diagnosis of growth hormone (GH) deficiency and central hypothyroidism at 4 years of age. We also diagnosed GH deficiency in one other patient. Joustra et al.[17] reported 3 patients with GH deficiency together with CH, but when GH secretion was reevaluated in two

Table 1. Patients with C-CH detected by neonatal screening in Sapporo city during 2004 to 2008

Patient	Diagnosis	Brain anomaly	FT4 at screening (ng/dL)	TSH at screening (U/L)
1	Prader-Willi		0.78	<0.5
2	MPHD (TSH, GH, LH, FSH, PRL, ACTH)	Hypo AP, Ectopic PP, Right optic nerve atrophy	0.75	1.3
3[a]	TSH deficiency	Normal	0.68	1.2
4	MPHD (TSH, GH, ACTH)	Hypo AP, Ectopic PP	0.96	3.2
5	MPHD (TSH, GH)	Ectopic PP, Invisible stalk	0.62	3.1
6	MPHD (TSH, GH)	Invisible stalk, Bilateral optic nerve atrophy	0.75	3.3

C-CH, Congenital central hypothyroidism; FT4, free thyroxine; TSH, thyroid-stimulating hormone; MPHD, multiple pituitary hormone deficiency; GH, growth hormone; LH, Luteinizing hormone; FSH, follicule stimulating hormone; PRL, prolactin; ACTH, adrenocorticotropic hormone; Hypo AP, hypoplasia of anterior pituitary gland; Ectopic PP, ectopic posterior pituitary gland.
[a]C-CH of the patient 3 was caused by immunoglobulin superfamily member 1 deficiency.

patients at adolescence, it was shown to be normal. It is possible that untreated hypothyroidism may impair GH secretion. Alternatively, because IGSF1 is expressed in somatotropes[14], an IGSF1 defect in these cells may affect GH secretion.

Four of our 5 patients had low levels of prolactin. The Dutch study found that 16/24 had hypoprolactinemia[17]. Thus, prolactin deficiency is one of the clinical features of IGSF1 deficiency.

Because TSH-based neonatal screening cannot identify patients with IGSF1 deficiency, treatment with thyroxine is delayed in those patients undergoing TSH screening. Therefore, there is a concern that psychomotor development may be delayed by late onset of treatment. However, several family members of affected patients showed no symptoms and their hypothyroxinemia was mild[14,17]. Their intelligence quotient seemed to be within the normal range. By contrast, in our study, one patient whose treatment was started at 4 years of age showed slightly delayed development[16]. Thus, it is still possible that severe cases of IGSF1 deficiency might be accompanied by developmental delay. Three of our patients did have delayed puberty and their serum luteinizing hormone and FSH levels remained at prepubertal levels even at 12 years of age. In the report of Sun et al.[14], 10 of 11 evaluated patients showed delayed testosterone production and pubertal growth. Delayed secondary sex characteristics may therefore be one of the clinical hallmarks in patients with pathogenic *IGSF1* mutations. In addition, testicular enlargement after adolescence is a characteristic feature of IGSF1 deficiency. It has been reported that all such patients aged more than 12 years manifested macroorchidism. In our study, two patients showed increased testicular size at 13 years of age (14 mL according to the Prader orchidometer) but one other had normal sized testes at 17 years of age. It has been suggested that testicular size increases from young to late adulthood. Thus, in this case testicular size may be increased in the future. Despite macroorchidism, fertility of male patients is likely to be normal[14,17].

We performed a TRH test twice in one patient. Compared with the result of the first TRH test, serum TSH was markedly reduced in the second test[16]. It has been observed that in *Igsf1* knockout mice, pituitary TSH synthesis and secretion are reduced, and pituitary TRH receptor mRNA expression is decreased[14]. It was speculated, therefore, that reduced TRH receptor signaling might be one of the pathogenic mechanisms of C-CH in *IGSF1*-deficient patients. TRH signaling through the TRH receptor is known to be an important factor for normal proliferation of thyrotropes[29,30], so in patients with IGSF1 defects, their proliferation during postnatal development may be impaired. This may indicate that IGSF1 is involved in thyrotrope proliferation and differentiation, in addition to TSH secretion (Fig. 1).

Joustra et al.[17] have analyzed metabolic parameters of children and adolescents with IGSF1 deficiency. They found that body mass index (BMI) was increased in 3 of 7 patients, and percentage of fat was high in 5. In adult cases, most patients showed increased BMI and fat, but this is not likely to be due to hypothyroidism, because patients who were treated from early infancy also showed these findings, as well as untreated individuals. This may suggest that obesity is not caused by hypothyroidism but rather a direct effect of IGSF1 deficiency itself. In our studies, the BMI of three patients was 18.5, 24.0, and 25.2 kg/m^2 at 12 years of age. Two patients showed higher BMI for their age than normal Japanese children[31], and thus careful follow-up for metabolic parameters is also necessary in IGSF1 deficiency.

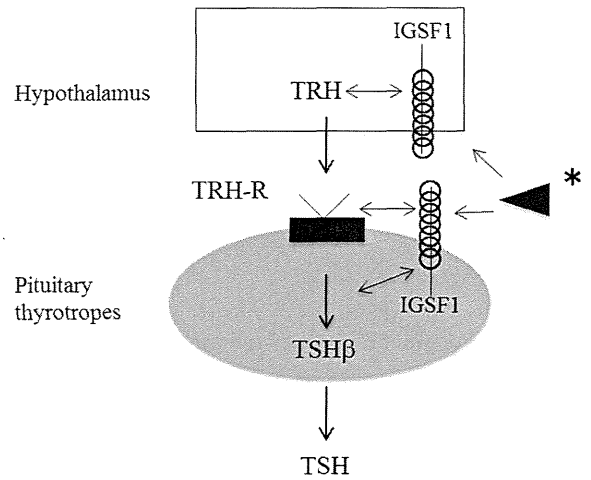

Fig. 1. Speculated function of IGSF1 in pituitary TSH synthesis and secretion. IGSF1 is likely to affect TSH synthesis, secretion and pituitary TRH receptor function. In addition, as IGSF1 is also expressed in hypothalamus, IGSF1 may affect TRH secretion. IGSF1, immunoglobulin superfamily member 1; TSH, thyroid-stimulating hormone; TRH, thyrotropin-releasing hormone. *, Arrowhead indicates that undetermined IGSF1 ligand may interact with IGSF1 on cell surface, and thus may modulate TRH-TRH receptor signaling.

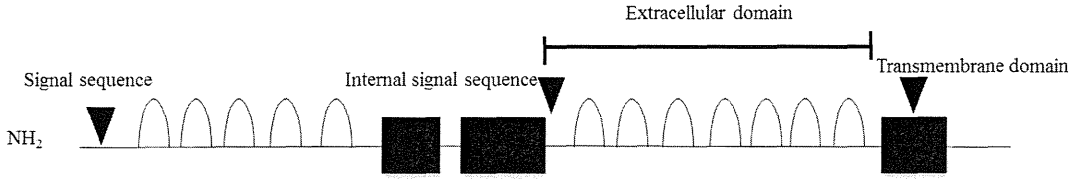

Fig. 2. Schematic representation of immunoglobulin superfamily member 1.

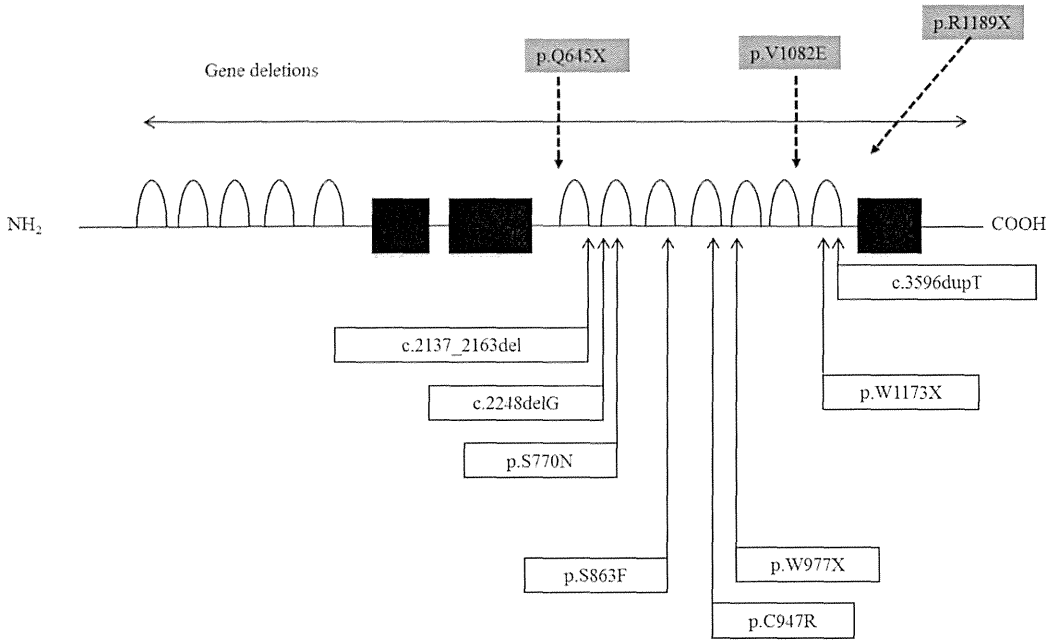

Fig. 3. Mutations/deletions of immunoglobulin superfamily member 1. Shaded boxes represent mutations we have described.

Mutations/deletions of *IGSF1*

Sun et al.[14] identified 8 distinct mutations and 2 deletions in IGSF1 in 11 families (Fig. 2). The mutations included in-frame deletions, single nucleotide deletions, nonsense mutations, missense mutations and one base duplication. *In vitro* expression studies of several mutations to analyze the functional consequences demonstrated that the encoded proteins migrated predominantly as immature glycoforms and were largely retained in the endoplasmic reticulum, resulting in decreased membrane expression[14]. In Japanese patients, we have reported two nonsense mutations, one missense, and one base insertion mutation (Fig. 3). In addition, a large deletion and a splice junction mutation have been identified (unpublished data). Two patients had the R1189X mutation. From interview, they were not related, but they lived in the same prefecture and thus this mutation may be a founder effect. We also performed an in vitro study and found that the V1082E mutated product was severely impaired in its posttranslational modification and membrane trafficking, similar to results of S770N, S863F and C947R, which were previously reported.

It is likely that there is no clear genotype-phenotype correlation. Even in familial cases sharing the same IGSF1 defects, a variable degree of hypothyroidism was observed[14,17]. Other genetic or environmental factors may influence the phenotypic expression of IGSF1 deficiency.

Conclusions

IGSF1 deficiency is a newly-discovered cause of C-CH. The physiological role of IGSF1 is unknown, and when clarified in future, its role in the mechanisms responsible for a variety of symptoms such as hypothyroidism, PRL deficiency, macroorchidism and delayed puberty will be clearer. IGSF1 is important for the pituitary-thyroid axis and the development puberty and thus represents a new player controlling growth and puberty in childhood and adolescence.

Conflict of interest

No potential conflict of interest relevant to this article was reported.

Acknowledgments

We thank Tomoyuki Hotsubo from Department of Pediatrics, NTT East Hospital and Toru Yorifuji from Department of Pediatrics Osaka City Medical Center for Children for data of patients. We also thank Beata Bak, Jessica Lam, and Daniel J. Bernard from Department of Pharmacology and Therapeutics, McGill University for fruitful discussion and in vitro analysis of IGSF1.

References

1. LaFranchi SH. Newborn screening strategies for congenital hypothyroidism: an update. J Inherit Metab Dis 2010;33(Suppl 2):S225-33.
2. LaFranchi SH. Approach to the diagnosis and treatment of neonatal hypothyroidism. J Clin Endocrinol Metab 2011;96:2959-67.